Modelling sphalerite mineral chemistry – towards a geometallurgical model for Gamsberg North

W. Price[1], A. Molifie[2], K. Pillay[2], K. Moses[2], I. Lipton[3], P. Greenhill[3], L. Torres[3], P. Spathelf [1], and M. Becker[2]

[1]Vedanta Zinc International, South Africa
[2]University of Cape Town, South Africa
[3]AMC Consultants Pty Ltd, Australia

Gamsberg North is a world class Zn ± Pb and Ag deposit located in the Northern Cape Province of South Africa that came into production in 2018. It is a geologically, geochemically and mineralogically complex ore deposit, with its primary variability arising from the complex Mn and Fe deportment. The primary ore mineral: sphalerite, exhibits a range of compositions depending on the degree of Fe and Mn substitution for Zn in the sphalerite crystal lattice. Mn in the flotation concentrate significantly impacts the price and saleability of the final concentrate product. To ensure that targets for the Mn grade in the final sphalerite concentrate are met, complex blending of the run of mine feed ore is required. This blending in turn requires upfront knowledge of the elemental composition of the sphalerite spatially throughout the ore body. This paper describes the programmatic approach that was taken to acquire this ore body knowledge using a range of analytical techniques (QEMSCAN, SEM-EDS/WDS, EPMA, XRD, Raman, ICP-OES) complemented by the application of machine learning algorithms to develop predictive models that can be applied to the drill hole database. Developing a comprehensive understanding of the mineralogy and associated sphalerite compositional variation across the orebody and host rocks is fundamental to managing various aspects of mining, through ore blending to the processing of the ore, to optimising the saleable concentrate.

INTRODUCTION

With the urgent global shift towards sustainability, decarbonisation and use of renewable energy resources, mining will play an increasingly important role in the supply of metals needed to implement the required technologies. In the case of Zn, which is used extensively in galvanising (thereby extending product life) and can also contribute to green energy (battery) storage, demand is expected to continue to rise (Watari *et al.*, 2021, Wang *et al.*, 2021). In combination with recycling initiatives, mining operations will be pressed to meet the expected demand for Zn (Rostek *et al.*, 2023). For a mining operation to maximise the endowment of an ore deposit, upfront knowledge is required of the geochemical, mineralogical and textural variability of the deposit and the effects of these on downstream processing and metallurgical performance – a concept encompassed by geometallurgy.

Numerous geometallurgy case studies have been published over the last few decades including useful reviews on geometallurgy highlighting its value and applications, e.g. Dominy *et al.,* (2018), Hunt *et al,.* (2019), Hunt and Berry (2017). However, for this study, the focus is more on the emerging trend of machine learning in geometallurgical applications where it has been used to predict both primary and response variables from readily available, inexpensive input data. For example, Mena Silva *et al.*, (2020) used the bulk chemistry of a nepheline syenite (industrial minerals) deposit to predict mineral grades and concentrate yield with artificial neural networks. Barker *et al.*, (2021) similarly predicted mineral grades using micro-XRF drill core data analysed with random forest algorithms.

The predicted mineral grades were used to support the interpretation of long wave infrared drill core spectra on a Carlin type gold deposit. Bhuiyan *et al.*, (2019) also used random forests to predict bond work index using a combination of geochemistry, geophysical and geomechanical drill core data as input variables. Machine learning using multivariate polynomial regression has also been used to predict mineral chemistry using a combination of electron probe micro analysis (EPMA) and bulk chemistry to predict the valuable Li content of micas (Wang *et al.*, 2022). In the case of this study at Gamsberg North, predicting the valuable and deleterious element content of the primary ore mineral, sphalerite, and the bulk mineralogy are the main geometallurgical focus.

Gamsberg North is a sediment hosted, strata-bound and metamorphosed sedimentary-exhalative Zn-Pb-Ag deposit. The deposit is stratigraphically placed in the Bushmanland Group and is classified as an Aggeneys Broken Hill-type deposit. The Gamsberg North deposit is located on the western flank of the Gamsberg Inselberg, which is formed from a large sheath fold structure (Figure 1). Mineralisation is hosted within the Hotson Formation or 'Aggeneys Ore Formation', which comprises a lower metapelitic unit and an upper, chemogenic Banded Iron Formation unit. The Gamsberg North mineralised body is formed from a range of metamorphosed exhalative chemical sediments, including manganiferous iron formations. Mineralisation is stratiform/strata-bound and semi-massive-to disseminated in nature, with the sulphide minerals (primarily pyrite-pyrrhotite) affected by polyphase deformation under upper amphibolite facies metamorphic conditions. The mineral of primary economic interest at Gamsberg North is sphalerite and to a lesser extent galena and associated silver. Three different ore types are mapped (Figure 1), listed stratigraphically from youngest to oldest: chemogenic magnetite pyroxene ore (MPO), pyrrhotite-dominated pelitic ore (PEO-PO), and pyrite-dominated pelitic ore (PEO-PY).

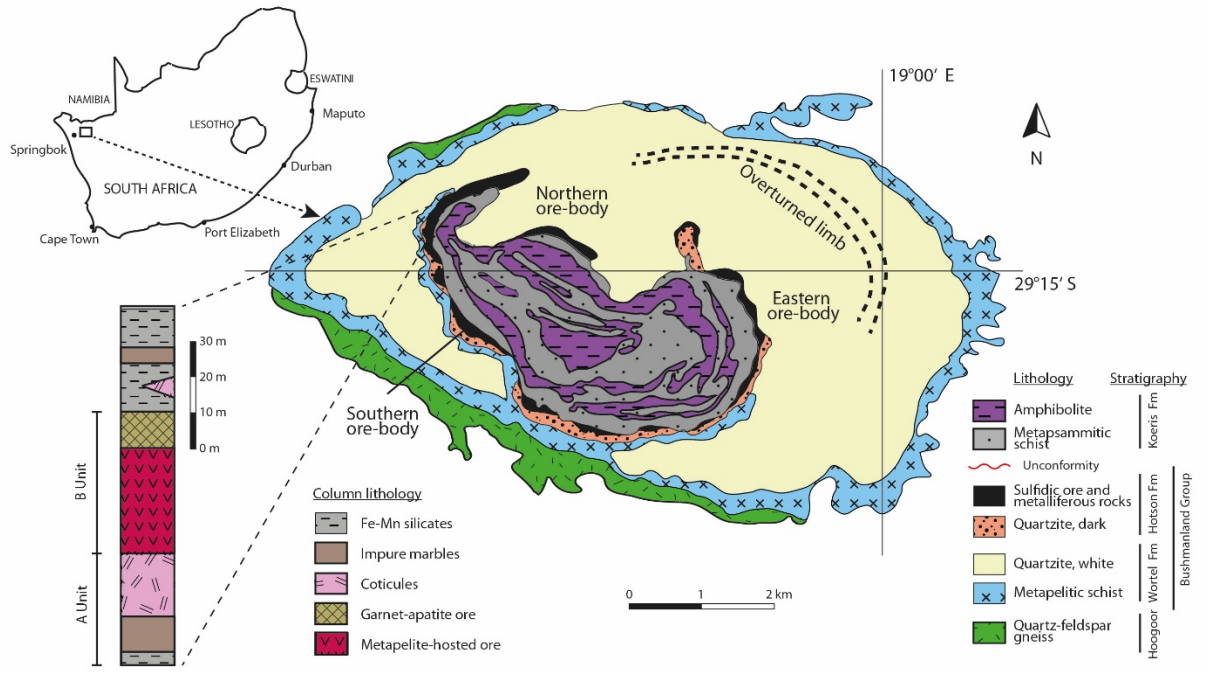

Figure 1. Geology of the Gamsberg deposit with the mineralised Hotson Formation shown in black. Adapted from: Höhn et al.*, (2021).*

Despite close to five decades of exploration, large scale open pit mining activities only formally commenced in 2015, with the newly built Gamsberg Zinc concentrator producing its first concentrate in 2018, and currently aiming to produce 265 kt metal in concentrate per annum. A second concentrator is under construction and plans are underway to develop an underground mine. One of the main reasons delaying the development of this resource since its discovery in 1972 is the geological, geochemical and mineralogical complexity of the ore. The primary variability arises from the complex Mn and Fe deportment (Schouwstra *et al.*, 2010) into both silicate (e.g. garnet, pyroxene, pyroxenoid)

and sulphide phases (sphalerite, alabandite). At Gamsberg, sphalerite compositions range from virtually pure ZnS (up to ~ 67% wt.% Zn) to Mn-Fe rich sphalerite (up to 20 wt.% Fe+Mn and 45 wt.% Zn) due to the substitution of Fe and Mn for Zn in the sphalerite crystal lattice (McClung and Viljoen, 2011). The presence of Mn in the flotation concentrate significantly impacts the price and saleability of the final concentrate product. Optimising the flotation circuit to minimise entrainment or depress unwanted gangue minerals will not adequately decrease the Mn grade because the majority of the Mn reporting to the concentrate is chemically bound in the sphalerite crystal structure. To ensure that targets for the Mn grade in the final sphalerite concentrate are met, complex blending of the run of mine feed ore is required. This blending in turn requires upfront knowledge of the sphalerite composition and mineral distribution spatially throughout the ore body.

The overarching objective of the project is to map the sphalerite composition and mineral grades of the Gamsberg North ore into a predictive geometallurgical model for ultimate use in mine planning and optimisation. A key priority of the predictive geometallurgical modelling was to obtain leverage from the tens of thousands of samples that comprise the drill hole database for the Gamsberg North deposit. This necessitated a systematic study, described here, to determine the most appropriate methods of collecting and modelling this information.

RESEARCH APPROACH

A programmatic approach was followed that initially focused on the collection of key analytical information at the required degree of confidence (building training datasets) before machine learning algorithms were used to model the desired geometallurgical variables. Quantitative evaluation of minerals by scanning electron microscopy (QEMSCAN) was initially used to determine the bulk mineralogy and sphalerite composition in phase 1 with 204 samples collected from drill holes in the Gamsberg North starter pit. Extensive characterisation results of one drill hole (Moses, In prep) were used to develop a method to determine sphalerite composition with QEMSCAN. A scoping study exploring the use of Raman spectroscopy as a potentially rapid drill core scanning tool to determine sphalerite composition was also included in phase 1. The follow-on study in phase 2 used a smaller set of only 15 samples and focused on the quantification and comparison of the errors in the determined sphalerite composition between scanning electron microscopy coupled with energy dispersive spectrometry (SEM-EDS), scanning electron microscopy coupled with wavelength dispersive spectrometry (SEM-WDS), and EPMA. Results from these two preliminary phases provided the necessary confidence in the strategy to be followed in phase 3, in which sphalerite mineral chemistry and bulk mineralogy were measured for 601 samples. Regression analysis and machine learning were thereafter used to model predictive relationships between mineralogical data and elemental assay data. The 601 samples analysed in phase 3 were used to train these predictive models. The models were then applied to the drill hole database using the regular sample assays.

Sampling and sample preparation

In phase 1, sub-75 µm pulverised material − which had already been split from aliquots sent for chemical assay by Gamsberg − was delivered to the University of Cape Town (UCT). In phases 2 and 3, quarter 47.6 mm and 63.5 mm diameter drill core samples were sent to UCT for further staged size reduction to ~ 65% passing 75 µm, carefully avoiding over milling to reduce the generation of excessive fines. Using a series of rotary rifflers, representative aliquots were split out for elemental assay, QEMSCAN and quantitative XRD (X-ray diffraction).

With the aim of gaining short-term value from this project, the bulk of the samples collected in phase 3 were selected within the next 3-4 years of the mine plan and spread across the entire strike extent of the deposit, which exceeds 1.2 km. The majority (571) of the samples came from the primary area of interest (Gamsberg North), whereas the remaining samples were selected from three drill holes from three Zn deposits along strike, namely Gamsberg Kloof, Gamsberg East and Gamsberg South, with the aim of determining the variability between Gamsberg North and these proximal deposits. The samples were selected from the three ore types in similar volumetric ratios that the ore types occur in the deposit to

ensure representativity. In addition to taking samples from the adjacent deposits, a small number of samples were selected from weakly mineralised rock types in the immediate hanging wall and foot wall of the mineralisation, as well as a highly localised internal waste unit.

Elemental and mineralogical analysis

Elemental analyses were conducted by ALS Modderfontein via inductively coupled plasma optical emission spectrometry (ICP-OES). Samples were prepared for analysis using 4-acid digestion.

For the QEMSCAN analysis, a 2 g aliquot for each of the samples was mixed with nanocarbon and resin to create 30 mm diameter blocks. After curing, the blocks underwent a series of grinding and polishing steps before carbon coating prior to QEMSCAN analysis. Samples were analysed on a FEI QEMSCAN 650F at UCT. Samples were analysed at 25 kV and 10 nA using the bulk mineralogical analysis measurement. Samples were run at 200X magnification and a 3.0 µm pixel size. A 3.5 g aliquot from one in every ten samples was micronised in ethanol before XRD analysis on a Bruker D8 diffractometer with LynxEye detector. CoKα radiation was used, with a scan range of 5 - 70° 2θ. Phase identification was performed using the Bruker EVA software, followed by phase quantification by the Rietveld refinement method using the Bruker TOPAS software package. The QEMSCAN datasets were validated by comparison of the QEMSCAN measured mineral grades with the QXRD determined mineral grades, as well as the QEMSCAN back calculated elemental grades with the ICP-OES measured elemental grades.

The composition of sphalerite was determined in four different ways – three by direct measurement using either EPMA, SEM-EDS or SEM-WDS. EPMA analyses in phase 1 were conducted on a Jeol JXA8100 Superprobe run at 25 kV and 20 nA at UCT. EPMA analyses in phases 2 and 3 were conducted on a Cameca SX100 probe at 25 kV and 40 nA at the University of Johannesburg. SEM-EDS analyses were run on the same QEMSCAN FEI 650F instrument using two Bruker 6130 EDS detectors interfaced with the Bruker Esprit software, and a standardless set up. SEM-WDS were run at Stellenbosch University on a Zeiss EVO instrument operating at 20 kV and 19 nA. For both the EPMA and SEM-WDS analyses a series of naturally occurring mineral and pure metal materials were used for standardisation. The fourth method was based on teaching the QEMSCAN software to classify sphalerite into different classes based on counts of metal ratios (e.g., Mn/(Fe+Zn) and applying a unique composition to each sphalerite class based on a fit-for-purpose calibration curve. The same polished 30 mm diameter QEMSCAN polished blocks were used for the different techniques for direct comparison. Raman analyses of sphalerite in phase 1 were collected using a WITec instrument at UCT with 532 nm laser excitation module and UHTS300 spectrometer VIS-NIS connected to a standard binocular light microscope.

RESULTS AND DISCUSSION

The key findings from phases 1 and 2 are presented to show important learnings that informed subsequent decisions for phase 3. To determine the composition of sphalerite, a calibration curve was developed for QEMSCAN, using both the EPMA measured concentrations of Zn, Mn and Fe, coupled with the QEMSCAN measured counts of Zn, Mn and Fe determined from equivalent grains in unbroken drill core (Figure 2a). At first glance the data looked promising but when applied to pulverised drill core samples two major issues were faced. The first related to the degree of scatter caused during EDS analysis of ultrafine (sub-10 µm) particles in the pulverised samples which does not lend itself to the generation of high-quality X-ray data, and the second related to the detection limits for Mn. Under the standard QEMSCAN measurement settings (1000 counts per pixel) Mn concentrations in sphalerite for Zn-rich, Mn poor sphalerite samples (below ~ 1 wt.% Mn) were below the detection limit. Despite optimising the QEMSCAN instrument settings (increasing counts per pixel), no significant improvements were noted. Because accurate information of Mn concentration in sphalerite was a priority, the focus was shifted away from QEMSCAN as the primary data source for sphalerite composition.

In phase 2, focus was first placed on ensuring particulate samples were not so finely pulverised and that a greater proportion of particles were of suitable size for high quality X-ray analyses. Subsequent

analyses of multiple grains from the same individual sample blocks with SEM-WDS and SEM-EDS, as well as using the EPMA dataset from phase 1, allowed a comparison of relative error of the analyses. Despite having the lowest number of grains analysed, the average relative standard error (RSE) for S, Mn, Fe and Zn was the smallest in the EPMA dataset (Table I). Figure 2b further illustrates the dependency of the relative standard error of Mn with sphalerite Mn concentration. With Mn concentrations below 1 wt.%, the SEM-EDS and SEM-WDS errors were particularly high (up to 100% RSE for one of the SEM-EDS samples), whereas the EPMA analyses varied between 4.1 and 15.5 % RSE. Based on this data, the decision was taken that the EPMA would be the desired instrumentation used to measure sphalerite composition in subsequent phases of work.

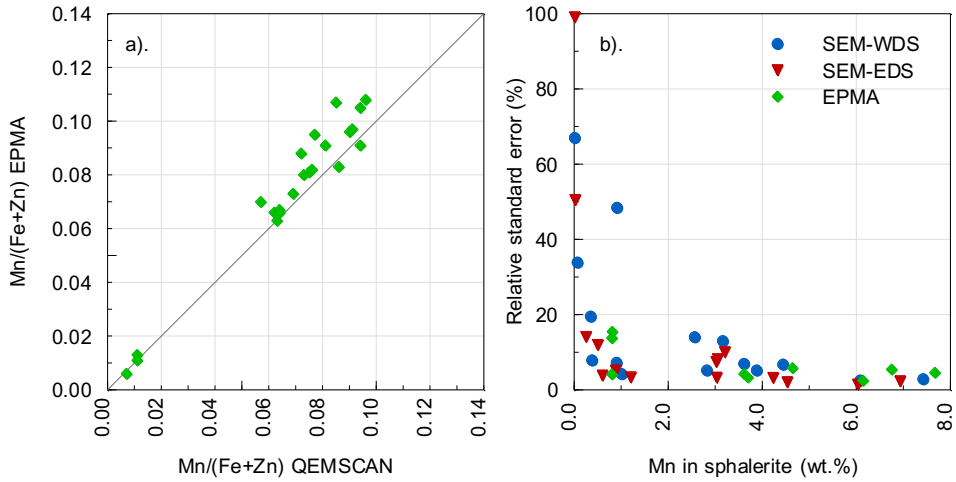

Figure 2. (a) Comparison of Mn/(Fe+Zn) ratios between EPMA and QEMSCAN for equivalent grains from unbroken drill core in phase 1 (drill core data from (Moses, In prep)). The y=x line is also shown. (b) Comparison of the dependency of the relative standard error on the Mn content of sphalerite as measured using SEM-EDS, SEM-WDS and EPMA.

Table I. Comparison of the average relative standard error for the determination of S, Mn, Fe and Zn in sphalerite dependent on the analysis method used

Method	No grains per sample	S	Mn	Fe	Zn
SEM-WDS	21	0.22%	16.31%	3.15%	0.79%
SEM-EDS	50	0.35%	15.77%	1.98%	0.47%
EPMA	10	0.29%	6.59%	1.67%	0.76%

A scoping study was also performed in phase 1 using Raman spectroscopy. The technique is based on the inelastic (Raman) scattering of phonons as they interact with an incoming monochromatic light source and can be used as a unique 'fingerprint' of different minerals. Many sulphides are Raman sensitive, including sphalerite, and previous studies have shown the sensitivity of the technique to mineral composition (e.g. Jiménez-Sandoval *et al.*, 2003, Osadchii and Gorbaty, 2010). The measurements are conducted at room temperature, without the need for a vacuum and the technique lends itself as a potential routine drill core scanning technology. Using the same 30 mm diameter blocks where the actual compositions of sphalerite were determined by EPMA in unbroken drill core, Raman data was collected. In Figure 3, it is evident that all sphalerite grains show the characteristic LO peak (vibrations parallel to the light source) at 356 cm^{-1} with the most Zn-rich sphalerite grains having the highest peak intensity. The characteristic TO peak (vibrations transverse to the light source) of pure sphalerite was notably absent on account of the Fe and Mn substitution in Gamsberg sphalerite. Two impurity mode peaks are present: at ~305 and 334 cm^{-1}. The intensity of both these peaks shows a correlation with the impurity content whereby the most Fe and Mn rich sphalerite grains have the

lowest peak intensity. Quantitative comparison of the EPMA Fe and Mn content of individual sphalerite grains with Raman peak heights showed a very strong negative correlation for Fe and Fe+Mn ($R^2 > 80\%$) and a slightly weaker correlation to Mn (R^2 is 63%). This demonstrated that although the Raman technique was sensitive to the impurity content of the Gamsberg sphalerite, the technique was not able to sufficiently discriminate whether the impurity was Fe or Mn.

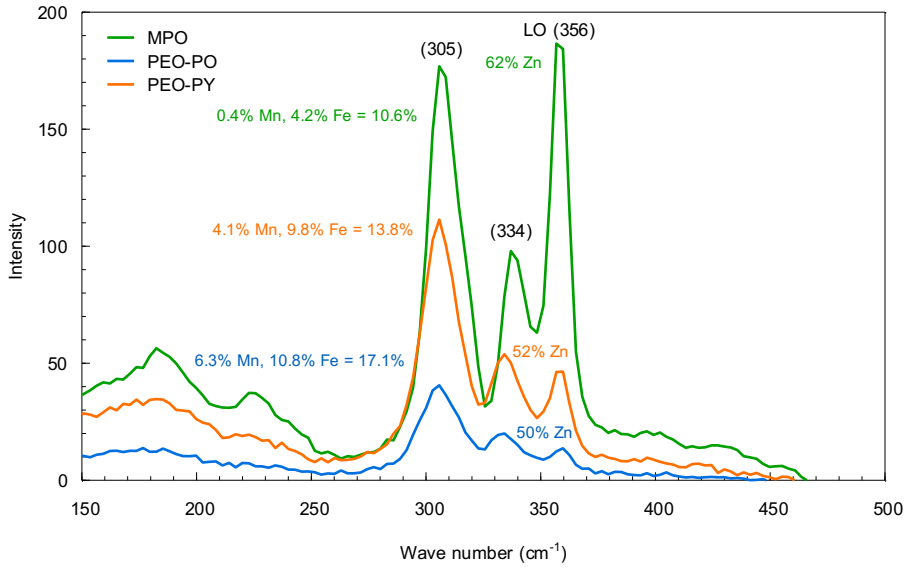

Figure 3. Raman spectra collected for selected Gamsberg sphalerite grains. The datasets are shown for sphalerite grains hosted in different lithologies, along with their EPMA measured compositions (in wt.%). The wave numbers of the key peaks at 305, 334 and 356 cm^{-1} are highlighted.

Data analysis and machine learning

The data provided by the phase 3 mineralogical analysis is summarised in Table II. The R open-source environment for statistical computing and the Python programming language were used for data analysis and machine learning.

Table II. Summary of datasets used for machine learning

Data type	Description
Meta data	Drill hole number, sampling interval, lithology, 601 samples
Geochemistry	4-acid digestion ICP-OES analysis with 35 elements, 601 samples
Sphalerite composition	EPMA, 15 grains per sample, Zn, Fe, Mn, Cd, S, 601 samples
Bulk mineralogy	QEMSCAN, 601 samples and Quantitative XRD, 60 samples

Sample representativity

The representativity of the geometallurgy samples was checked by comparing the multivariate distribution of the geometallurgy samples with the ore samples in the whole drill hole database. Because it is difficult to compare high-dimensional data using conventional one-, two- or three-dimensional graphs, the Uniform Manifold Approximation and Projection (UMAP) dimension reduction algorithm was applied to the multivariate data so that it could be viewed in a 2D projection. UMAP is an advanced mathematical technique widely used in data science (McInnes *et al.*, 2018). UMAP was chosen for this study as it better preserves local and global structure than many other algorithms and can be applied to multiple data sets. Figure 4 shows the drill hole samples and the geometallurgy samples plotted according to the first two vectors of the UMAP transformation. The plot shows that the two data sets

have similar coverage in multivariate space. Conventional statistical comparisons confirm this observation. Therefore, predictive models developed using the geometallurgical samples as the training data set should be appropriate for deployment to the drill hole database, in samples where all the required independent variables are available.

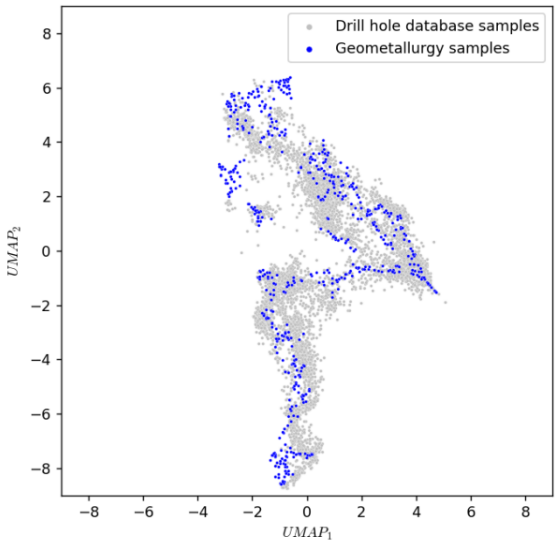

Figure 4. Gamsberg North drill hole database samples and the 601 geometallurgy samples plotted according to the first two vectors of the UMAP transformation.

Exploratory data analysis

Exploratory data analysis was carried out to identify key features, relationships and patterns in the data that could be exploited for predictive modelling. Scatter plots were used to check for non-linear relationships and outliers. Outliers in data can be problematic for machine learning algorithms. There were 15 instances (2.5%) of the data considered as outliers that were subsequently excluded from further analysis. From the exploratory data analysis, seven numerical features, Al, Ca, Fe, Mg, Mn, Zn, S, and the categorical Lith feature were nominated as independent variables for prediction of sphalerite composition.

The EPMA data set comprises a snapshot of the composition of the elements Zn, Fe, Mn, Cd and S in 15 grains of sphalerite from each of the 601 samples. The EPMA data is compositional: the five elements are not independent. The mean total compositional value (the sum of Zn, Fe, Mn, Cd and S) is 99.2%. There is a clear alignment of Zn, Fe, and Mn in a three-dimensional trend surface. Six data points which were divergent from this trend were removed from subsequent regression modelling. After the data cleaning there were 580 EPMA records (337 PEO_PY, 171 PEO_PO and 72 MPO).

Approach to regression modelling

Building regression models for each EPMA measurement independently would not necessarily satisfy the compositional constraint for the combined predictions. Therefore regression models where generated, using the following stepwise algorithm: (i) Calculate the total of the elements measured by EPMA for each sample; (ii) Given the set of nominated independent variables, predict Zn in sphalerite by regression; (iii) To force the compositional constraint, normalise the Fe, Mn, and S to the difference between the total EPMA assay and the Zn prediction; (iv) Predict Fe by regression; (v) Normalise the Mn and S to the difference between the total EPMA assay and the sum of predicted Zn and Fe; (vi) Predict Mn by regression; (vii) Predict S as the residual of the total EPMA assay and the sum of predicted Zn, Fe and Mn; and (viii) Check that the sum of predictions displays the same statistical distribution of the total EPMA assay.

Supervised machine learning was used for regression modelling. Three regression models were tested with the stepwise algorithm: linear regression (LR), the Cubist model (Quinlan, 1992) and a projection pursuit regression (PPR) model. Cross-validation checks were carried out applying random splits of data for training and validation.

LR was used as the initial candidate and benchmark for modelling. In linear regression, established as an optimisation problem, the goal is to find the parameter values, or coefficients, that minimise the quadratic sum of data values versus model estimates, in a classical ordinary least squares problem estimation. The Cubist model incorporates decision trees with multivariate linear regression along with ensemble learning and allows for adjustment of estimates using the k nearest neighbours from the training data. This method was chosen as it can deal with non-linearity in the data using decision trees and boosts the accuracy of a single multivariate linear regression equation through additional models (committees). The resulting models are more complex than simple linear regression, tend to be more accurate than standard ordinary least squares linear regression, and can be interpreted because the model consists of a set of if-then-outcome (linear regression) rules. Ensemble learning is a powerful method of training multiple models on different parts of the data set. The approach takes advantage of the wisdom of the crowd where the average of multiple models tends to be more accurate than any single model. The technique also helps to minimise the risk of over-fitting by training multiple models on different parts of the data. It also allows more complex and generally more accurate models to be trained on limited data where over-fitting of the data would otherwise occur. PPR can also handle cases where there are non-linear relationships between the independent variables The key aspect of PPR models is the application of a linear projection pursuit transformation to the independent variables. This transformation focuses on finding projections in the high dimensional space of the data features that deliver useful information (Friedman and Stuetzle, 1981). PPR works by adding several linear combinations of smoothed projections. Each individual projection of the independent variable is smoothed to capture the main trend in the relationship between the transformed independent variable and the target variable.

Supervised machine learning was also used to predict the sphalerite, pyrrhotite, and pyrite content of the samples (alabandite was ignored since it only occurred in negligible amounts). The QEMSCAN data, ICP-OES assays for Al, Ca, Fe, Mg, Mn, Zn, and S, and the categorical feature Lith were used to train LR, Cubist, and PPR regression models. For proof of concept, the ICP-OES features were assumed to be independent (i.e., non-compositional).

Regression modelling results

In all cases the compositional structure of the predicted sphalerite components was maintained. Figure 5 shows scatter plots of the predicted versus actual Zn, Fe, Mn, and S concentrations in sphalerite using the different regression models. The results predicted using the ordinary least squares regression are very poor and are conditionally biased. The results predicted using the Cubist model perform well for Zn, Fe and Mn and have high R^2 (coefficient of determination) values whereas the S prediction is relatively poor but unbiased. Compared to the Cubist model, the PPR predictions of Zn and Mn are further improved, with only minor loss of accuracy in the Fe predictions. The S predictions remain relatively poor but unbiased. The relative inaccuracy of the S predictions arises because the errors in the predictions of Zn, Fe and Mn (including the analytical errors in both the dependent and independent variables) accumulate in the residual value that is used to calculate the S prediction. In terms of economic importance, the S content is the least important of the four predicted element grades.

The scatter plots given in Figure 6 show the predicted versus actual mineral grades for sphalerite, pyrite and pyrrhotite. The Cubist and PPR models consistently outperformed the LR models and produced very high R^2 values (generally greater than 0.8). The PPR results show the highest R^2 values.

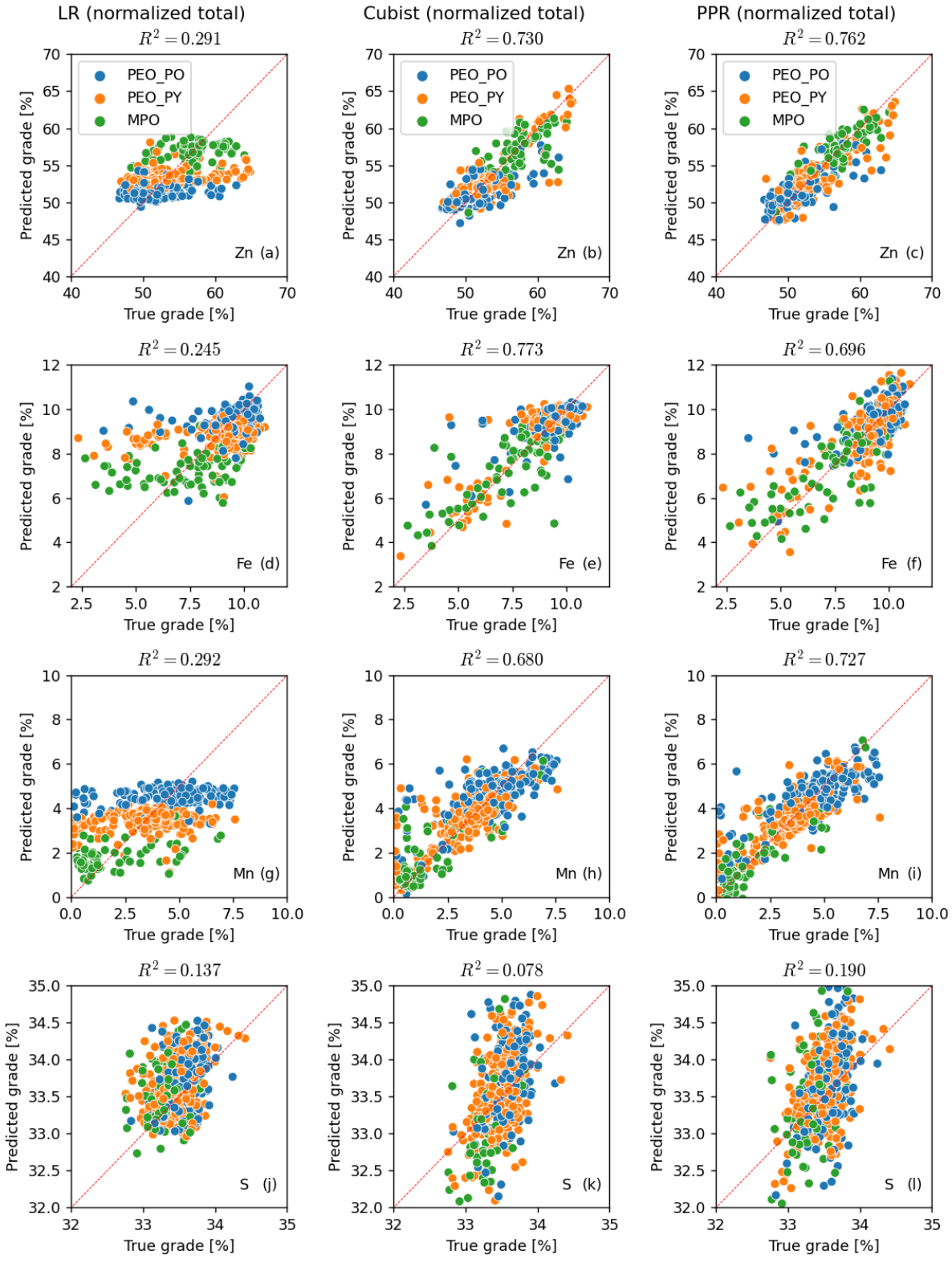

Figure 5. Scatter plots of the predicted versus actual Zn (a-c), Fe (d-f), Mn (g-i) and S (j-l) concentrations in sphalerite using least squares regression, Cubist model and the project pursuit regression model. The accompanying R^2 is also given.

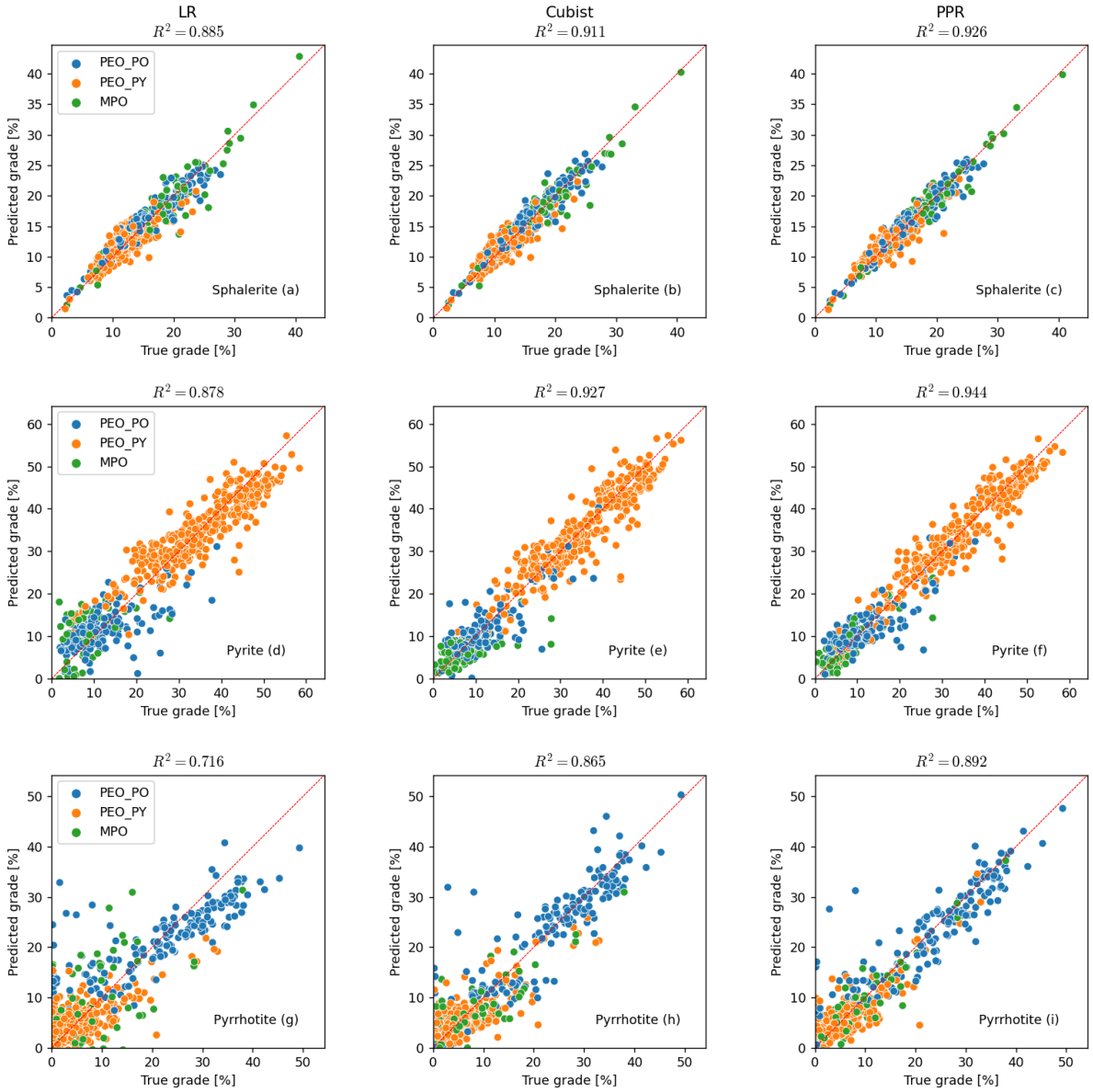

Figure 6. Scatter plots of the predicted versus actual mineral grades for sphalerite (a-c), pyrite (d-f) and pyrrhotite (g-i) using least squares regression, Cubist model and the project pursuit regression model. The accompanying R^2 is also given.

Application of the predictive mineralogy models

Predictive models were deployed to the drill hole sample database. For the sphalerite composition, Cubist models were deployed for prediction of Zn, Fe and Mn concentrations, with S calculated as the residual. For the mineral grades all three methods produced reasonable results for sphalerite, pyrrhotite and pyrite, so LR was deployed because it is simpler. For the other minerals, Cubist models were deployed. The predictions of sphalerite quality were reviewed in Cartesian space. The conclusion is that the predicted sphalerite chemistry matches the current lithological and structural understanding, with Zn-rich sphalerite in the upper portion of the mineralised package (related to the MPO) and Zn-poor sphalerite towards the base, related to the pelitic ores. The combination of statistical validation and spatial validation indicates that the predictions of sphalerite quality are reasonable.

The drill hole samples were composited into 2 m intervals whereafter the predicted sphalerite quality

variables were estimated into the resource blocks using the Inverse Distance Weighting method, with the estimation being controlled by domain boundaries. Figure 7 shows the resultant model with clear sub-parallel domains of Zn-rich and Zn-poor sphalerite, which non-coincidentally follow the plunge of the orebody, again supporting the conclusion that the predictions are reasonable.

The geometallurgical model is currently undergoing final testing prior to formal deployment. It is envisioned that the benefits of the geometallurgical block model will include: (i) Improvements to stockpiling strategy and management – current stockpiling is solely based on mining area (a proxy for sphalerite composition in the absence of additional data), whereas further stockpiling can be based on the predicted sphalerite composition; (ii) Improvements in mine scheduling – ensuring concurrent mining takes place in different areas, allowing an acceptable final concentrate product to be delivered; and (iii) Changes in the run of mine blending strategy – blending to allow predictable sphalerite recoveries, to ensure final flotation concentrate grades are within acceptable parameters and to ensure effective use of the concentrator, preventing excessive reagent consumption and equipment wear.

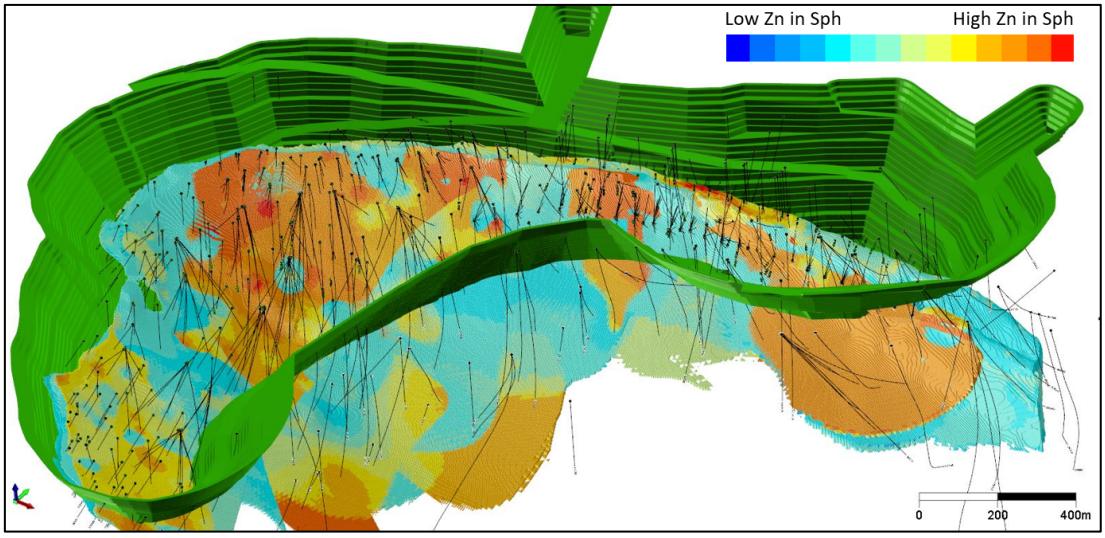

Figure 7. Zinc concentration of sphalerite in the geometallurgical model in relation to final open pit design.

CONCLUSIONS

This study has demonstrated that QEMSCAN analysis can be extended to the quantitative prediction of mineral composition in an orebody but was not suitable for the estimation of sphalerite composition at the required level of accuracy (particularly for Zn-rich, Mn-poor sphalerite). EPMA provided the mineral specific compositional data necessary for the prediction of sphalerite composition. Used in tandem, these two techniques provide a powerful suite of tools when coupled with machine learning techniques to improve orebody knowledge.

Subsequent work demonstrated that it is possible to achieve reasonable predictions of sphalerite composition and ore mineral grades, by applying data science and machine learning techniques, including regression modelling, to the elemental assay data that has been routinely collected for exploration and resource definition. The predictive models can also be applied to any new drill holes that are added to the database.

The data analysis and machine learning formed a preliminary study sufficient to demonstrate that useful predictions could be made. There is scope to optimise the selection of independent features and parameters used for the predictive models, apply transformations to address the compositional data, and apply the predictions to future versions of the resource block model. This would allow the geometallurgical estimates to be seamlessly embedded in all mine planning and production scheduling work at Gamsberg North.

ACKNOWLEDGEMENTS

Grateful thanks to various members in the Centre for Minerals Research who performed the sample preparation and assisted in redrawing Figure 1; to ALS Modderfontein for the ICP-OES data, and to Christian Reinke from the University of Johannesburg for the electron probe microanalyses. Acknowledgements to Markus Schaefer and Jaco Smit who helped initiate the project concept with VZI.

REFERENCES

Barker, R. D., Barker, S. L. L., Cracknell, M. J., Stock, E. D. and Holmes, G. 2021. Quantitative Mineral Mapping of Drill Core Surfaces II: Long-Wave Infrared Mineral Characterization Using µXRF and Machine Learning. *Economic Geology,* 116**,** 821-836.

Bhuiyan, M., Esmaieli, K. and Ordóñez-Calderón, J. C. 2019. Application of data analytics techniques to establish geometallurgical relationships to bond work index at the Paracutu Mine, Minas Gerais, Brazil. *Minerals,* 9**,** 29-29.

Dominy, S. C., O'Connor, L., Parbhakar-Fox, A., Glass, H. J. and Purevgerel, S. 2018. Geometallurgy—A route to more resilient mine operations. *Minerals,* 8**,** 1-33.

Friedman, J. H. and Stuetzle, W. 1981. Projection Pursuit Regression. *Journal of the American Statistical Association,* 76**,** 817-823.

Höhn, S., Frimmel, H. E. and Price, W. 2021. Syn-metamorphic sulfidation of the Gamsberg zinc deposit, South Africa. *Mineralogy and Petrology,* 115**,** 709-728.

Hunt, J., Berry, R., Becker, M. and Baumgartner, R. 2019. A special issue dedicated to geometallurgy: Preface. *Economic Geology,* 114**,** 1473-1479.

Hunt, J. A. and Berry, R. F. 2017. Geological Contributions to Geometallurgy: A Review. *Geoscience Canada,* 44**,** 103-103.

Jiménez-Sandoval, S., López-Rivera, A. and Irwin, J. C. 2003. Influence of reduced mass differences on the Raman spectra of ternary mixed compounds: $Zn_{1-x}Fe_xS$ and $Zn_{1-x}Mn_xS$. *Phys. Rev. B,* 68**,** 54303-54303.

McClung, C. R. and Viljoen, F. 2011. A detailed mineralogical assessment of sphalerites from the Gamsberg zinc deposit, South Africa: The manganese conundrum. *Minerals Engineering,* 24**,** 930-938.

McInnes, L., Healy, J. and Melville, J. 2018. UMAP: Uniform manifold approximation and projection for dimension reduction. *arXiv preprint arXiv:1802.03426*.

Mena Silva, C. A., Ellefmo, S. L., Sandøy, R., Sørensen, B. E. and Aasly, K. 2020. A neural network approach for spatial variation assessment – A nepheline syenite case study. *Minerals Engineering,* 149**,** 106178.

Moses, K. In prep. *Mineralogical and geochemical characterisation of the Gamsberg Zinc deposit, South Africa.* PhD, University of Cape Town.

Osadchii, E. G. and Gorbaty, Y. E. 2010. Raman spectra and unit cell parameters of sphalerite solid solutions ($Fe_{1-x}Zn_xS$). *Geochimica et Cosmochimica Acta,* 74**,** 568-573.

Quinlan, J. R. Learning with continuous classes. *In:* Adams, A. and Sterling, L., eds. Proceedings of 5th Australian Joint Conference on Artificial Intelligence, 1992 Hobart, Tasmania. World Scientific, 343–348.

Rostek, L., Pirard, E. and Loibl, A. 2023. The future availability of zinc: Potential contributions from recycling and necessary ones from mining. *Resources, Conservation & Recycling Advances,* 19**,** 200166.

Schouwstra, R., De Vaux, D., Hey, P., Malaysiak, V., Shackleton, N. and Bramdeo, S. 2010. Understanding Gamsberg - A geometallurgical study of a large stratiform zinc deposit. *Minerals Engineering,* 23**,** 960-967.

Wang, L., Su, C., Wang, L.-Q., Zhangzhou, J., Xia, Q.-K. and Wang, Q.-Y. 2022. Refined estimation of Li in mica by a machine learning method. *American Mineralogist,* 107**,** 1034-1044.

Wang, N., Wan, H., Duan, J., Wang, X., Tao, L., Zhang, J. and Wang, H. 2021. A review of zinc-based battery from alkaline to acid. *Materials Today Advances,* 11**,** 100149.

Watari, T., Nansai, K. and Nakajima, K. 2021. Major metals demand, supply, and environmental impacts to 2100: A critical review. *Resources, Conservation and Recycling,* 164**,** 105107.

Prof Megan Becker
Associate Professor
University of Cape Town

Associate Professor Megan Becker leads the geometallurgy and process mineralogy research activities in the Centre for Minerals Research, and the Minerals to Metals Initiative in the Department of Chemical Engineering at the University of Cape Town. Her research interests focus on understanding the effects of mineralogy on minerals processing, metallurgy and the environment, and how best mineralogy information be articulated and communicated to maximise the value of minerals to society.

Since joining the Centre in 2005, she has successfully integrated process mineralogy into the research activities of the Centre and other research groupings within the Dept of Chemical Engineering. A highlight was her establishment of a state-of-the-art facility for quantitative mineralogical analysis hosting a R15 million FEI 650F FEG QEMSCAN – quantitative evaluation of minerals through scanning electron microscopy in 2014. She has also conceptualised, designed, developed and run courses in process mineralogy at both the undergraduate student level and industry professional development level.

She has close to 100 peer reviewed publications. After having recognised the complete non-existence of relevant references texts on process mineralogy in 2011, she initiated a Monograph on Process Mineralogy. She was the lead editor of this Monograph, published in 2016 through the Julius Krutschnitt Mineral Research Centre. The text contains over 30 peer reviewed chapters written by international experts in the field of process mineralogy.

Ian Lipton

Principal Geometallurgist
AMC Consultants Pty Ltd

40 years of experience in mining geology, resource evaluation, geometallurgy, and exploration, covering a wide range of commodities and mining operations. Ian is responsible for designing and managing geometallurgical studies to reduce risk and improve outcomes in feasibility studies and operating mines. He has been involved in a variety of geometallurgical projects predicting ore processing response characteristics for commodities such as gold, copper, lead-zinc, nickel and iron ore. Ian is an authority on density measurement and the author of a variety of technical papers on resource estimation, density, mining geology, and geometallurgy. He has presented Mine Geology and Grade Control, and Geometallurgy training courses to professionals in Australia, Sweden, Tanzania, Brazil and Indonesia.